Geomechanics and Engineering, *Vol. 32, No. 3 (2023) 335-346*
https://doi.org/10.12989/gae.2023.32.3.335

Passive p-y curves for rigid basement walls supporting granular soils

Imad Elchiti[a], George Saad[b] and Shadi S. Najjar*

Department of Civil and Environmental Engineering, American University of Beirut, P.O. Box 11-0236 Riad El-Solh 1107-2020, Lebanon

(*Received July 22, 2020, Revised January 15, 2023, Accepted January 18, 2023*)

Abstract. For structures with underground basement walls, the soil-structure-interaction between the side soil and the walls affects the response of the system. There is interest in quantifying the relationship between the lateral earth pressure and the wall displacement using p-y curves. To date, passive p-y curves in available limited studies were assumed elastic-perfectly plastic. In reality, the relationship between earth pressure and wall displacement is complex. This paper focuses on studying the development of passive p-y curves behind rigid walls supporting granular soils. The study aims at identifying the different components of the passive p-y relationship and proposing a rigorous non-linear p-y model in place of simplified elastic-plastic models. The results of the study show that (1) the p-y relationship that models the stress-displacement response behind a rigid basement wall is highly non-linear, (2) passive p-y curves are affected by the height of the wall, relative density, and depth below the ground surface, and (3) passive p-y curves can be expressed using a truncated hyperbolic model that is defined by a limit state passive pressure that is determined using available logarithmic spiral methods and an initial slope that is expressed using a depth-dependent soil stiffness model.

Keywords: passive pressure; plaxis; p-y curves; rigid walls; soil-structure interaction

1. Introduction

1.1 Background

For structures with basement walls, the soil-structure-interaction (SSI) between the side soil and walls affects the response, particularly under cyclic loading. In the context of performance-based design, there is interest in quantifying the relationship between the lateral earth pressure and wall displacement using the concept of p-y curves by replacing the homogeneous soil continuum by a series of springs that mimic the soil behavior adjacent to the substructure. The p-y method is advocated by geotechnical/structural engineers in the design of laterally loaded piles (Matlock 1970, Reese *et al.* 1974, API 1993). The problem for piles has been extensively studied using full scale field tests, centrifuge tests, and 3D finite element analyses (Wilson *et al.* 2000, Boulanger *et al.* 1999).

Various studies have investigated the response of retaining walls under static and seismic loading conditions (Gazetas *et al.* 2016, Mikola *et al.* 2016, Conte *et al.* 2017, Bakr and Ahmad 2018, Dilmac *et al.* 2018). On the other hand, very limited studies have been conducted on the mobilization of lateral earth pressure behind rigid walls in the context of p-y curves. Briaud and Kim (1998) were the first to recommend p-y relationships for the analysis and design of tieback walls. These p-y relationships were calibrated/back calculated using data collected from full scale tests on walls in sand. Briaud and Kim (1998) state that the lateral earth pressure that is exerted by the soil on the wall is bounded by the active and passive earth pressure conditions. Based on the data collected, they recommend that the active pressure could be assumed to be mobilized at wall movements of 1.3 mm (away from the retained soil) and the passive earth pressure at wall movements of 13 mm (into the retained soil). El Ganainy and El Naggar (2009) and Saad *et al.* (2016) adopted this p-y relationship as the backbone curve for the lateral pressure-lateral deflection relationship used for modeling the side soil in their analysis of buildings.

P-y curves were also incorporated in the analysis of lateral SSI for walls under dynamic loading. In the dynamic analysis, the near-field soil (in contact with the wall) is customary modeled by a series of link elements (springs) with an axial stiffness that is characterized by a given p-y curve. Richard *et al.* (1999) modeled the near-field soil by a series of springs having a bilinear p-y curve consisting of an elastic portion bounded by upper and lower limits defined by active and passive limit states, respectively. The elastic stiffness of the near-field soil was modeled by $k_s = 1.35G_z/H\sqrt{z/H}$, G_z being the shear modulus of the soil at a depth z, H the height of the wall, and z the depth at which the p-y response is being modeled. Maleki and Mahjoubi (2010) used the same p-y model for defining the stiffness of the spring elements in the study of the effect of wall flexibility on the soil resistance during dynamic loading.

In reality, the relationship between lateral earth pressure and wall displacement is expected to be complex and is

*Corresponding author, Associate Professor
E-mail: sn06@aub.edu.lb
[a]Post-Doctoral Researcher
E-mail: imadelchiti@gmail.com
[b]Associate Professor
E-mail: gs31@aub.edu.lb

ISSN: 2005-307X (Print), 2092-6219 (Online)

affected by the height of the wall, the relative density of the backfill material, the interface friction between the wall and the soils, the non-linearity of the soil response, and the type of wall movement (translation and/or rotation). Elchiti *et al.* (2017) conducted a preliminary investigation of the p-y response of rigid basement walls in the active state of loading and concluded that the above-mentioned complexities in the relationship between lateral earth pressure and wall displacement could be captured using numerical analyses. The analyses conducted in Elchiti *et al.* (2017) were restricted to rigid basement walls that are simplistically assumed to be fixed at their base (supported on rock) and subjected to active loading.

Numerical results from soil structure interaction analyses conducted in Saad *et al.* (2016) on buildings with underground stories indicated that the maximum base shear at the ground level was governed by the lateral earth pressures mobilized in the retained soil behind the wall during seismic excitation. In particular, the lateral soil stresses that were mobilized as the wall was pushed towards the soil (passive loading direction) dictated the design base shear needed for the design of the shear walls. These results point to the need for realistic models that could describe the p-y relationship for rigid retaining walls to be used as input in robust soil-structure-interaction problems in the context of performance-based design. Such p-y relationships could be incorporated in commercial structural analysis software in the form of non-linear springs that describe the lateral pressure versus lateral displacement relationship. This is consistent with the p-y curves concept commonly used to model the reaction of the soil for laterally loaded piles.

The goal of this paper is to shed light on the mechanics of the soil-structure interaction between rigid basement walls and granular backfill soil in the passive state of loading. This is achieved by (1) building a PLAXIS 2D model that incorporates the wall, backfill soil and foundation soil (2) investigating the effect of the height of wall, soil properties, and interface friction angle on the lateral p-y response, and (3) utilizing the numerical results to establish a simple empirical model that is capable of predicting the p-y response behind rigid basement walls in the passive state of loading. It should be noted that while the assumption of "full rigidity" may not be ideal, it is the most representative of the expected lateral behavior of basement walls with underground stories.

2. Finite element model

2.1 Plaxis 2D model

The finite element model (FEM) of the rigid retaining wall and the backfill material was built in PLAXIS 2D and presented in Fig. 1. The model consisted of four elements: a rigid wall, a semi-infinite half-space backfill soil, a semi-infinite half space subsoil, and an interface soil layer acting as a soil-wall boundary. The rigid wall was modeled as a rectangular plate element. The wall is moved incrementally in the passive direction using a trapezoidal prescribed displacement field. Differential displacement between the top and bottom of the wall results in a combined rotational/translational wall movement. The horizontal prescribed displacement also ensures that no vertical movement or bending of the plate element can occur. A rotation/translation wall movement was chosen based on the results presented in Saad *et al.* (2016) for basement wall displacements under real earthquake excitations. The study revealed that walls in buildings that included multiple basements showed more-or-less rigid wall rotations with maximum lateral wall displacements recorded at the top of the basement wall (ground level) and minimum lateral wall displacement recorded at the level of foundations. The magnitude of the horizontal wall displacement at the foundation level was evaluated to be between 5% and 20% of the top wall displacement.

Six-node plane strain triangular elements were used to mesh the subsoil and backfill continua. The finite element mesh was adaptively refined to converge to an element distribution with sizes ranging from fine triangular elements at locations of stress concentration at the wall-soil and soil-soil interfaces to course elements at the boundaries. Moreover, an interface layer was constructed at the soil-wall boundary and at the backfill-subsoil boundary. Modeling an interface layer at the boundary of two materials is desirable for several reasons. It allows for the reduction in soil strength and soil stiffness at the interface as well as for the formation of differential displacement (slippage) between the adjoining elements thus minimizing stress build-up at points of stress concentration. Interface layers in PLAXIS are modeled as rectangular elements with zero thickness. The property of the interface layer in PLAXIS is given through a reduction factor R_{int}. At the soil-wall interface, R_{int} was varied in accordance with the parametric study presented in the following section, while at the soil-subsoil interface, a value of 1.0 was selected.

The left and right boundary conditions of the finite element model are selected to limit horizontal movements due to applied wall displacement while simultaneously allowing free vertical displacement at the boundaries. The bottom subsoil boundary is modeled as a full fixity. The length of the retained soil and the depth of the subsoil layer are selected following a comprehensive sensitivity analysis. Inadequate length of the retained soil will result in the formation of back pressure at the backfill boundary. Several lengths of soil ($6H_w$, $10H_w$, $15H_w$, and $20H_w$) were investigated in the sensitivity analysis. Significant magnitudes of back pressure were observed for the backfill length of $6H_w$. However, back pressure magnitudes dropped significantly with an increased backfill length of $10H_w$ and became negligible at a backfill length of $15H_w$ and non-existent for a backfill length of $20H_w$. As a result, a $20H_w$ backfill soil was used in the study. A similar analysis was done for determining the required depth of the subsoil layer. The sensitivity analysis revealed that a subsoil depth of $3H_w$ is sufficient to minimize boundary effects.

The effect of bottom wall translation on passive p-y response was investigated assuming bottom wall displacements that are 5%, 10%, and 20% of the top wall displacement. This range of bottom wall displacements is consistent with numerical results presented in Saad *et al.*

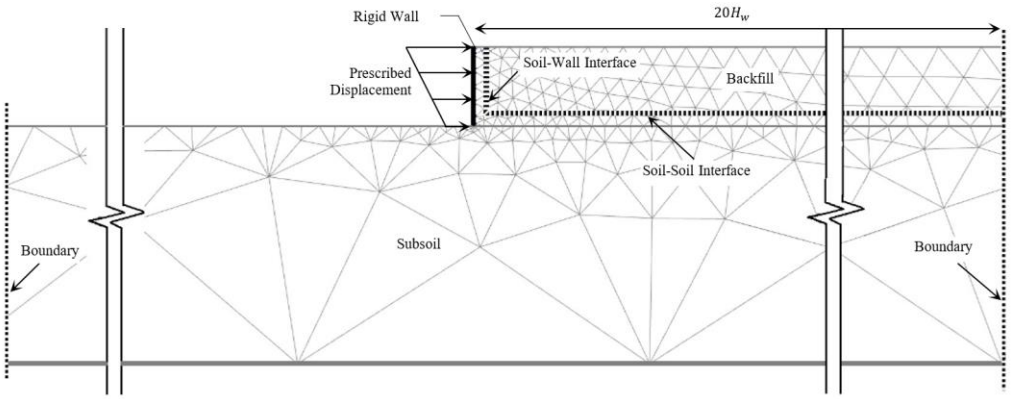

Fig. 1 Finite element model in Plaxis 2D

(2016) for full scale reinforced concrete buildings that are subjected to earthquake shaking. The effect of the assumed bottom wall displacement on the numerically derived p-y curves is presented in Fig. 2 for a 10 m wall retaining medium-dense sand. The p-y curves are presented for depths ranging from 1 to 7 m. The results indicate that bottom wall displacements (y_b) with a magnitude ranging from 5% to 20% of the top wall displacement (y_t) have an insignificant effect on the p-y response. Based on these results, a decision was made to adopt a bottom wall displacement that is equal to 20% of the top wall displacement in the remainder of this study.

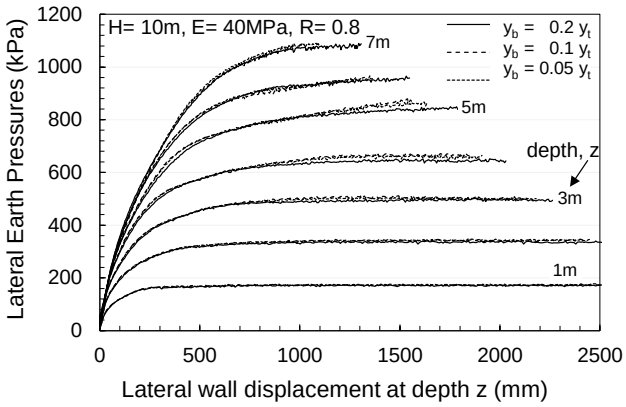

Fig. 2 Effect of bottom wall translation on p-y response

2.2 Constitutive soil model

Elchiti *et al.* (2017) compared the response of granular backfill in active wall displacement for the Mohr-Coulomb model and the more advanced Hardening Soil model available in PLAXIS. They concluded that the results of the Mohr-Coulomb model exhibit signs of numerical instability at relatively small wall displacements. These numerical instabilities were attributed to the elastic-perfectly plastic nature of the Mohr-Coulomb model, whereby soil elements in the passive failure wedge will yield early on in the deformation process therefore causing loss of numerical stability at larger deformations. On the other hand, the Hardening Soil model yielded a more stable response that could predict the p-y behavior of the retained granular soil up to large wall displacements. Accordingly, the Hardening Soil model was adopted to model the constitutive response of the backfill and subsoil.

The Hardening Soil model is an advanced non-linear model that assumes a hyperbolic relationship between stress and strain. The Hardening model adopts isotropic hardening and includes two yield surfaces to differentiate between shear and isotropic loading. The final bounding surface is based on the Mohr-Coulomb failure envelope with a non-associated flow rule using the dilatancy angle as the non-normality parameter. With respect to stiffness, the model considers stress and strain level dependency of the moduli. A hyperbolic stress-strain relation is considered between the deviatoric stress and the major principal strain to account for strain dependency, while a power law is adopted to consider stress dependency.. In this study, the parameters

Table 1 Soil properties in constitutive model

	Loose	M. Dense	Dense
Soil Unit Weight, $\gamma(kN/m^3)$	16.5	18.0	19.5
Soil Relative Density R_d *(%)*	45	67	84
Initial Void Ratio, e_{int}	0.685	0.615	0.560
Sec. Stiffness, $E_{50}^{ref}(MPa)$	15-25	30-50	60-80
Tang. Stiffness, $E_{oed}^{ref}(MPa)$	15-25	30-50	60-80
Unload/ reload Stiffness, $E_{ur}^{ref}(MPa)$	200000	200000	200000
Power of stress dependency of E, m	0.4	0.4	0.4
Cohesion, $C'_{ref}(kN/m)$	1.0	1.0	1.0
Friction Angle, $\emptyset'(°)$	33	36	39
Dilation Angle, ψ $(^o)$	4	7	11
Poisson' Ratio, ν'	0.3	0.3	0.3
Reference Stress, p_{ref} (kPa)	100	100	100
Failure Ratio, R_f	0.95	0.95	0.95

utilized in the Hardening soil model (Table 1) were adopted from Skeini (2015) for loose, medium and dense Ottawa sand. The water table was assumed to be deep. The subsoil was assumed to be a very dense sand ($\gamma = 20\,kN/m^3$, $e_{int} = 0.31$, $E_{50}^{ref} = 100\,MPa$, $m = 0.4$, $\emptyset' = 40°$, $\psi = 13^o$, and $R_f = 0.95$) so that it does not have an influence on the soil-structure interaction between the wall and the backfill.

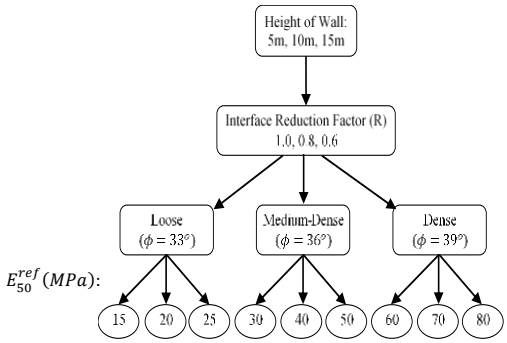

Fig. 3 Parametric study chart

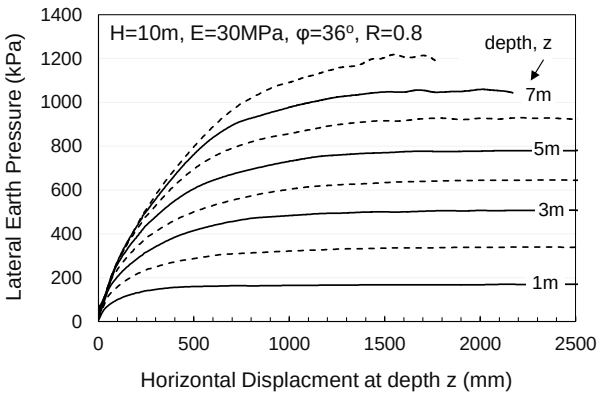

Fig. 4 Typical passive p-y curves

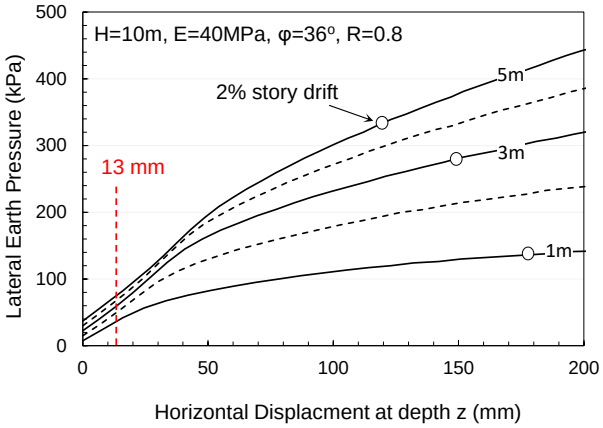

Fig. 5 P-y curves in the practical range of wall displacement

It should be noted that all interface soil layers in PLAXIS 2D are modeled using the Mohr-Coulomb model. When more advanced soil models are chosen, PLAXIS 2D extracts the parameters relevant to the Mohr-Coulomb model and applies the reduction factor to them to deduce the soil-wall and backfill-subsoil interface responses.

2.3 Parametric study

The results in this study are based on a parametric analysis that was designed and implemented to characterize the components that affect the variation of lateral earth pressure with respect to passive wall displacement. The parametric study consisted of varying (1) the height of wall, (2) the relative density (RD) of the soil and (3) the soil-wall interface reduction factor, R_{int}. Three wall heights, 5 m, 10 m, and 15 m, corresponding to 2, 4, and 6 basement floors, respectively, were considered. For each wall height, loose (RD = 45%), medium-dense (RD = 67%), and dense (RD = 84%) dry granular soils were considered as backfill material. The soil properties associated with each relative density are presented in Table 1. Three soil-wall interface reduction factors (0.6, 0.8, and 1.0) were considered in the investigation. These values were chosen to be in line with the common values used in practice for the case of granular soil bearing on concrete walls. A graphical representation of the above parametric study is shown in Fig. 3.

3. Numerically derived passive p-y curves

To construct p-y curves using the FE results, lateral earth pressures at 1-m depth intervals were extracted from stress points selected at the soil-wall interface and plotted against the horizontal wall displacement at that depth. Typical p-y curves for the case of medium-dense sand retained by a 10 m high wall having an interface reduction factor of 0.8 are shown in Fig. 4.

Several observations can be made based on the reported results. First, passive p-y curves exhibit a non-linear monotonic increase in lateral earth pressure ending in an asymptotic limit-state passive pressure. Second, there is a reduction in the rate of stress increase with increased wall displacement consistent with the reduction in the soil stiffness with increased strain for the hardening model used. Third, the rate at which passive pressure mobilizes behind the wall is sensitive to the embedment depth, z. P-y curves at shallower depths mobilize at faster rates than those at lower depths. This is observed by comparing wall displacement needed for the limit-state passive pressure to be reached at different depths below the ground, which shows that passive pressure is mobilized at y=600 mm and y=2000 mm for depths of 1 m and 5 m, respectively.

The large wall displacements needed for full passive pressures to be mobilized may not be reached in practical applications involving basement walls under real seismic shaking. Most building codes limit story-drift (y_t/H_w) to less than 2.0%, y_t being the top wall displacement and H_w the height of the wall. Consequently, for SSI problems, there is more value in characterizing the p-y response at relatively smaller displacements that may be attained in practice. Fig. 5 presents the early stages of the p-y response for the same wall. Wall displacements corresponding to 2% story drift at each depth z are marked by circles on the p-y curves. An investigation of the p-y curves in the lower displacement range indicates that non-linearity in the p-y response is clearly visible and is observed at early stages of wall displacement. This is essential for proposing future models for the prediction of p-y curves for performance-based design applications whereby story drift (lateral wall displacement) could be the governing design criteria.

Results on Fig. 5 indicate that the elastic-perfectly plastic p-y models that are being advocated in the literature (Briaud and Kim 1998, Richard *et al.* 1999, Maleki and

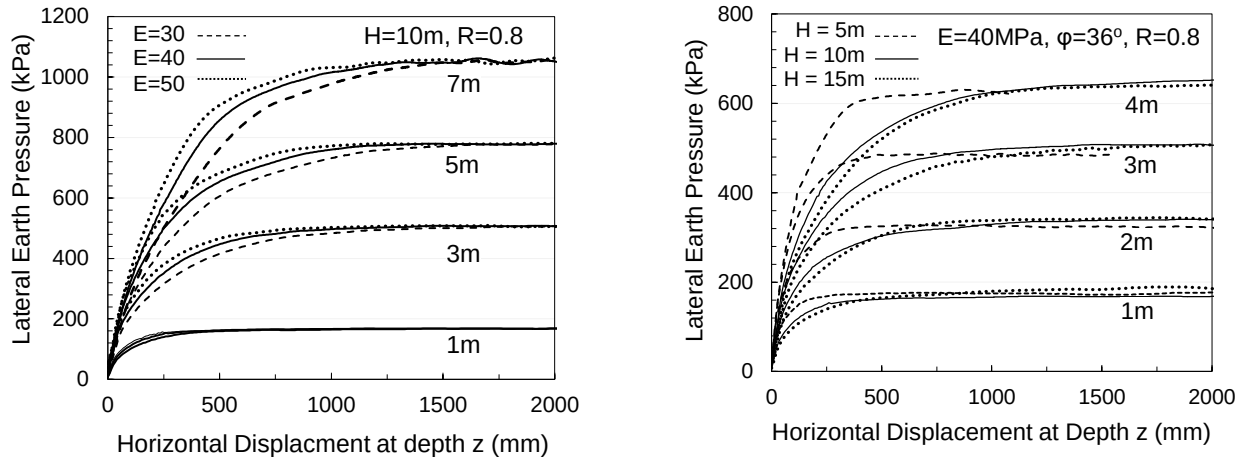

(a) (b)

Fig. 6 (a) effect of soil modulus on p-y response and (b) effect of wall height on p-y response

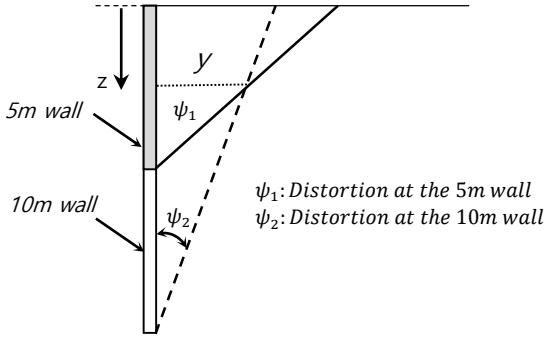

Fig. 7 Wall distortion for 5 m and 10 m walls for a given Displacement y at depth z

Mahjoubi 2010) are incapable of predicting the non-linear p-y curves without suffering from over-prediction of the lateral pressures at different levels of wall displacement. The adoption of a depth-independent fixed displacement of 13 mm as a criterion for mobilization of passive pressure in published p-y models may not be representative of the true response. The 13 mm criterion is clearly an early estimate for the development of full passive pressure.

The p-y curves in Figs. 4 and 5 correspond to the case of a 10-m wall that is supporting medium dense sand with a modulus of elasticity of 40 MPa. The effects of varying the stiffness of the backfill and the height of the wall on the resulting p-y curves are presented in Figs. 6(a) and 6(b), respectively. Results on Fig. 6(a) pertain to cases where the soil modulus (E) was varied between 30 and 50 MPa. The p-y curves indicate that sands with a lower stiffness lead to an initially "softer" p-y response, with lower mobilized lateral stresses at any given wall displacement.

As expected, the effect of "E" is restricted to the initial portion of the p-y curve with no impact on the maximum passive pressures at limit state. For any given depth, the curves converge at a common limit state pressure at large wall displacements. This observation is logical given that the maximum passive pressure is governed by the friction angle of the sand and the interface friction coefficient between the sand and the wall, and is independent of the initial stiffness, E.

The effect of wall height on the passive p-y response is shown in Fig. 6(b). P-y curves for wall heights of 5 m, 10 m, and 15 m retaining medium-dense sand for depths ranging from 1 m to 4 m are presented. Results indicate that cases with shorter walls exhibit a stiffer (steeper) initial p-y response. The stiffer response observed in the 5-m high wall cases at any wall displacement could be attributed to the larger distortion/shear strain that is expected in the soil retained by the shorter wall. An indicative sketch is presented in Fig. 7 to show the displacement/distortion conditions in 5 m and 10 m high walls that are displaced such that the local wall displacements (y) at a given depth z are equal in both walls. Define ψ_1 and ψ_2 as the angular distortions of the 5 m and 10 m walls, respectively (see Fig. 7). As indicated in the figure, for both walls to displace the same amount y at a given depth z, the 5 m-wall will have to undergo higher angular distortions compared to the 10 m-high wall. This will eventually result in the development of higher shear stresses and higher passive pressures in the shorter walls as portrayed in Fig. 6.

The parametric study was extended to study the effect of the interface reduction factor R on the observed p-y response. The interface reduction factor for granular soil bearing on poured concrete is commonly taken to be between 0.6 and 1.0. To study the effect of R, a 10 m rigid wall retaining medium-dense soil was analyzed for R values of 0.6, 0.8, and 1.0. P-y curves for depths ranging between 1 m and 7 m are plotted on Fig. 8(a). At any given depth z, results indicate that the three p-y curves corresponding to the three values of R initiate from the same at-rest pressure and end at three different values of limit-state passive pressures at large wall displacements. A negligible effect of the interface friction coefficient is noted with regards to the initial part of the p-y curves which represents relatively smaller wall movements. The p-y curves for different R values diverge at wall displacements ranging from 10 cm (for shallow depths) to around 40 cm (at larger depths). This divergence at relatively large displacements is expected since the limit-state passive pressure is correlated with the assumed interface reduction factor, R.

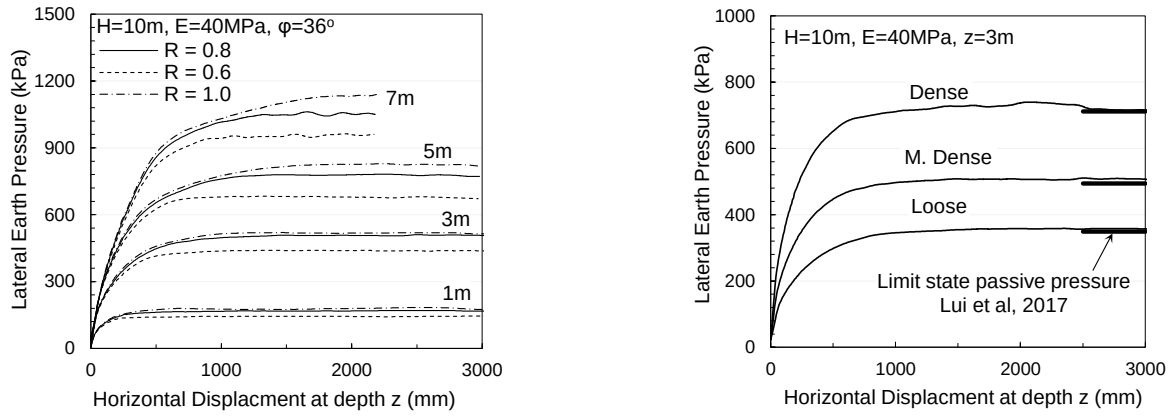

Fig. 8 The effect of (a) interface reduction factor R and (b) soil density on the p-y response

The results presented in Figs. 4, 5, 6, and 8(a) pertain to cases with medium dense sand. The effect of relative density of the retained soil on the p-y response is investigated in Fig. 8b for cases involving a 10-m high wall and an interface reduction factor of 0.8. Parameters representing each relative density are presented in Table 1 with soil moduli of 20 MPa, 40 MPa, and 70 MPa in the case of loose, medium-dense, and dense soil, respectively. The p-y curves in Fig. 8(b) point clearly to the significant effect of relative density on the p-y response. As expected, the cases with loose and medium dense sands show lower magnitudes of the limit-state passive pressure compared to the dense sand case. The effect of relative density is equally visible in the lower displacement range with stiffer responses observed in the case of dense sands.

Based on the parametric study, it could be concluded that the passive p-y response is affected by the depth below the ground surface z, the soil modulus E, the relative density, and the height of the wall H_w. On the other hand, the effect of the interface reduction factor R is confined to the p-y response at larger wall displacements.

4. Empirical p-y model

4.1 Model formulation

Several models were proposed in the literature for the prediction of p-y curves. The models vary in complexity and accuracy from simple elastic-perfectly plastic models (Briaud and Kim 1998) to more advanced non-linear models including power functions (Matlock 1970), nonlinear functions (API 1993, Ramberg and Osgood 1943, Duncan and Mokwa 2001) and piecewise linear models (Allotey and El Naggar 2007). P-y models that are based on the Ramberg-Osgood model were successfully employed in modeling p-y curves for piles under lateral loading. The Ramberg-Osgood model can be expressed as

$$p = \frac{(C_o - C_f)y}{\left[1 + \left\{\frac{(C_o - C_f)y}{p_f}\right\}^m\right]^{1/m}} + C_f y \qquad (1)$$

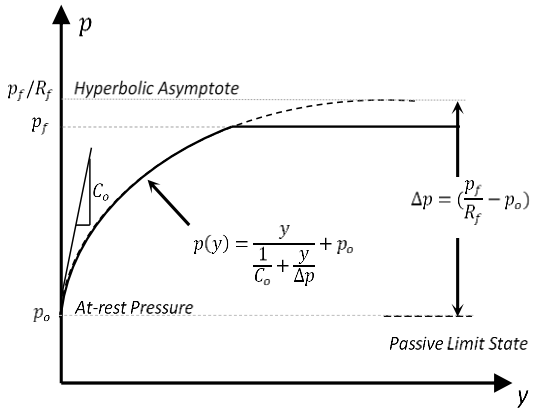

Fig. 9 Hyperbolic model for at-rest to passive response

Where C_o and C_f are the initial tangent spring stiffness and the spring tangent stiffness at failure, respectively, p_f is the spring force at the yield point, and 'm' is the order of the p-y curve. For the case of predicting passive pressure behind walls, the expected stiffness, C_f, at limit-state can be considered to be equal to 0. If m is taken as 1 and the lateral pressure at $y = 0$ is introduced into the equation as the at-rest value (p_o), the Ramberg-Osgood model in Eq. (1) can be simplified to

$$p = \frac{y}{\frac{1}{C_o} + \frac{y}{\Delta p}} + p_o \qquad (2)$$

where Δ_p is the change between the initial at-rest pressure p_o and the asymptotic pressure at failure p_f/R_f, and R_f is commonly introduced to minimize fitting errors. Duncan and Chang (1976) proposed a range for R_f between 0.75 and 0.95. A sketch representing the p-y model of Eq. (2) is shown in Fig. 9. When the expression for Δ_p is replaced in Eq. (2), the final form becomes

$$p = \frac{y}{\frac{1}{C_o} + \frac{y}{\frac{p_f}{R_f} - p_o}} + p_o \qquad (3)$$

The expression in Eq. (3) is one form of a hyperbola.

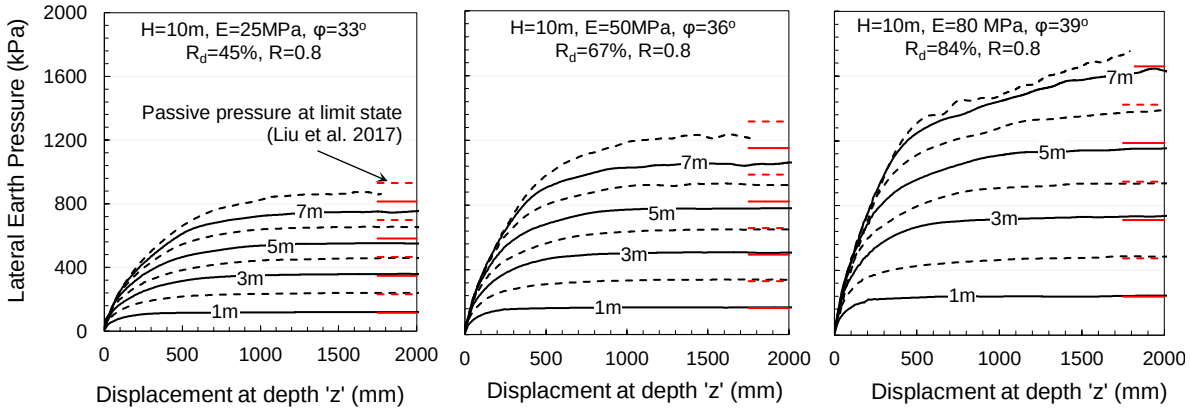

Fig. 10 Comparison between FE analysis and limit-state passive pressure proposed by Liu *et al.* (2017)

The use of this form of hyperbolic function for the prediction of p-y response is desirable for two reasons. First, it can replicate the shape of typical p-y curves that exhibit monotonic increasing pressures that tend to a defined horizontal asymptote at a decreasing rate. Second, they are easy to construct, requiring the determination the initial slope C_o and the value of the passive pressure at limit-state, p_f.

4.2 Passive pressure, p_f

Different approaches were proposed for the prediction of passive lateral stresses behind retaining systems. These include limit equilibrium methods (Rankine 1857, Coulomb 1776, Terzaghi 1943), upper and lower bound analyses (Chen 1975, Soubra and Regenass 2000), and finite element methods (Tejchman and Bauer 2007, Hanna *et al.* 2001, Hanna and Diab 2017). One of the earliest limit equilibrium approaches for calculating p_f was proposed by Rankine (1857) and Coulomb (1776). Rankine's theory predicts passive pressure accurately for smooth wall interfaces (δ=0) retaining horizontal backfill, while Coulomb's theory presents a more general solution allowing for the presence of a sloped backfill and a rough wall interface (δ>0).

Coulomb's theory overpredicts passive pressures for walls with δ > ϕ/2. As a result, Terzaghi (1943) proposed the use of a curved failure plane (logarithmic spiral) to enhance the prediction of passive pressure. His method was fine-tuned to include a composite failure plane consisting of a curved and straight segment (Kumar 2001, Rao and Choudhury 2005). Liu *et al.* (2017) proposed a modification to Terzaghi's method. They proposed a simplified method for the prediction of the non-linear failure plane. The failure plane consisted of a logarithmic spiral and a straight line failure zone. Using numerical and Mohr circle analyses, both failure zones were defined and the the passive resultant force (P_p) determined by solving an optimization problem. According to the author, this method led to good results for the case of granular soil and inconclusive results for the cohesive soils.

The method by Liu *et al*. (2017) was utilized to predict passive pressures for cases involving a 10-m wall with soils of different densities. The predictions are shown in Fig. 10 together with the numerically derived p-y curves for the cases under consideration. The passive pressures proposed by Liu *et al.* (2017) are shown as bold lines on the right side of each figure. Results indicate that the passive pressures that are predicted using the Liu *et al.* (2017) model compare well with the asymptotic pressures resulting from the FE analysis. At larger depths, there is a tendency for the model to slightly overestimate the numerically derived passive pressures at large deformations. This is more visible in the cases of loose and medium-dense soil. This discrepancy in the limit-state passive pressure could be attributed to the wall movement that was adopted in our numerical model. The Liu *et al.* (2017) method is based on pure uniform lateral translation of a gravity wall in contrast to the translation/rotation movement adopted in this study for the rigid reinforced concrete wall. It should be noted that this inconsistency should not impose a challenge when proposing an empirical p-y model that is based on Eq. (3). As stated previously, most design codes limit story drift to less than 2.0% making it unlikely for limit state passive pressures to fully develop behind the wall at practical depths. It could thus be concluded that the logarithmic spiral method proposed by Liu *et al.* (2017) is considered satisfactory for the current work and will be adopted for the prediction of passive pressures at the limit state.

4.3 Initial stiffness, C_o

The second parameter required for modeling p-y curves using the hyperbolic equation presented in Eq. (3) is the initial stiffness (C_o). Unlike the limit-state passive pressure p_f, there is very limited literature on C_o. The determination of C_o encompasses 1) extracting the values of C_o from the FE results, 2) quantifying the dependence between C_o and the main parameters $(z, E, H_w, \phi, \gamma)$ which were found to have an impact on the numerically derived p-y response as identified in Section 4, and 3) proposing a simplified model for the prediction of C_o.

4.3.1 Extracting C_o from the FE results

Clough and Duncan (1971) presented a methodology for determining the initial stiffness of a set of data points to be

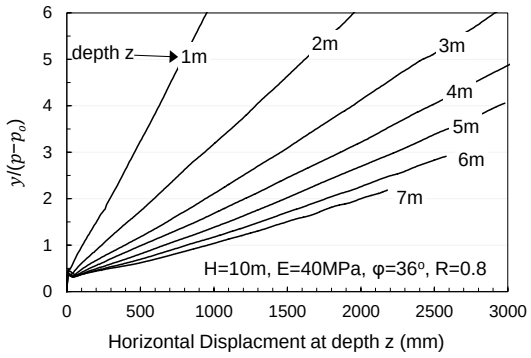

Fig. 11 P-y curves for 10m wall retaining medium dense soil transformed into straight lines using Eq. (5)

fitted by a hyperbolic function. In its general form, the hyperbolic function expressed in Eq. (3) can be written as

$$p = \frac{y}{b + ay} + p_o \tag{4}$$

By rearranging the variables, Eq. (4) can be transformed into a straight line through the following expression

$$f(y) = \frac{y}{p - p_o} = ay + b \tag{5}$$

Where a = 1/Δp and b = 1/C_o. The expression in Eq. (5) is that of a straight line with a slope 'a' and an intercept 'b'. Plotting the hyperbola as a straight line (Eq. (5)) will allow for determining the initial slope C_o as the reciprocal of the y-intercept. Fig. 11 shows p-y curves for a 10 m wall retaining medium dense soil transformed into straight lines using Eq. (5). The minor curvatures in the lines are explained by the slight mismatch between the fitting model and the data extracted from FE analysis. To account for this mismatch, Liu *et al.* (2017) proposed that each line be replaced by a line passing through two points (70% and 90% of the maximum stress). This would standardize the fitting procedure and reduce any subjectivity.

4.3.2 Sensitivity of C_o to Z, E, and H_w

Fig. 12 shows the variation of C_o with the depth of embedment z for loose, medium dense, and dense soil. The values of C_o at incremental depths of 1m were back calculated using the method described in Section 4.3.1. Results on Fig. 12 indicate that C_o increases with embedment depth at a decreasing rate, reaching a peak value at approximately mid height of the retaining wall.

After that depth, C_o is observed to stabilize with very minor reductions at depths approaching the bottom of the wall. The initial increase in the values of C_o with depth z is expected given the increase in the soil modulus with depth. In the hardening model, the soil modulus for granular soils (E_{50}) is expressed in terms of the vertical confinement pressure (σ_3) through the following equation

$$E_{50} = E_{50}^{ref} \cdot \left(\frac{\sigma_3}{p^{ref}}\right)^m \tag{6}$$

Where E_{50}^{ref} is the modulus of elasticity specified at a p_{ref} of 101 kPa, σ_3 is the confining pressure, and the power

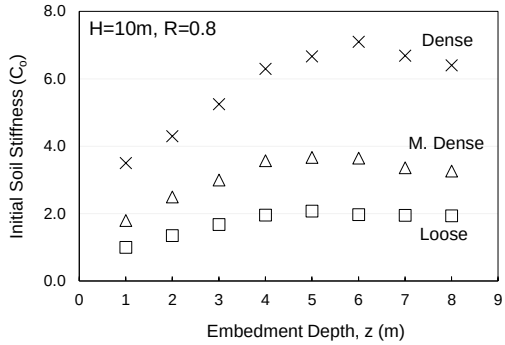

Fig. 12 C_o for a 10 m wall retaining loose (E=20 MPa), medium-dense (E=40 MPa), and dense soil (E=70 MPa)

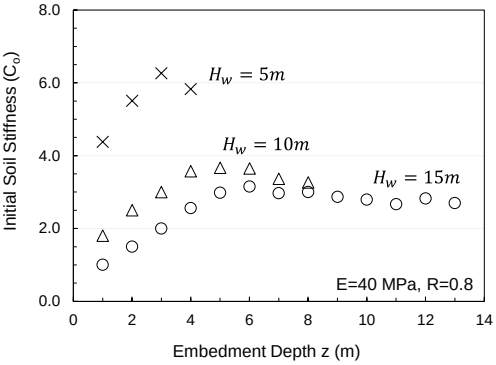

Fig. 13 Sensitivity of C_o to wall height H_w

factor 'm' defines the stress dependency on E_{50}. The peak that is observed in the relationship between C_o and z at depths beyond 0.5H_w is possibly caused by the rotational movement of the wall. Alternatively, this peak could be due to a soil arching phenomenon that could lead to reduction in stresses next to the wall with depth.

Fig. 13 presents the dependency of the initial stiffness C_o on the wall height H_w. The effect of wall height on the initial soil stiffness is clear in the sense that soils retained by shorter walls exhibit higher initial stiffnesses than those retained by higher walls. More importantly, the peak that is observed in the value of C_o around the mid-height of the wall is applicable, irrespective of the height of the wall.

This observation indicates that any attempt to model the variation of C_o with depth needs to incorporate the height of the wall and the increase in C_o with embedment up to a peak C_o value that is a function of the height of the wall.

4.3.3 Modeling the initial stiffness, C_o

In this section, a simplified numerical expression is proposed to model the variation of C_o with depth. The expression is based on a two-part model as indicated in Fig. 14. The first part consists of a non-linear curve (Eq. (7)) that is applied over the upper half of the retained soil (z between 0m and 0.5H_w). The second part of the model assumes a constant value of C_o determined by Eq. (7) at depth 0.5H_w.

$$C_o = E_{50}^{ref} \times \left(\frac{\gamma z}{p_{ref}}\right)^m \times \frac{1}{H_{eff}} \tag{7}$$

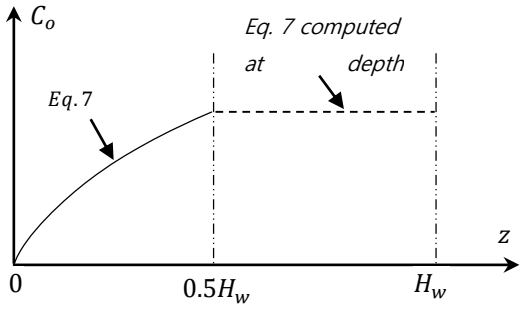

Fig. 14 Proposed model for C_o

(2017) model, the initial stiffness C_o is modeled using the

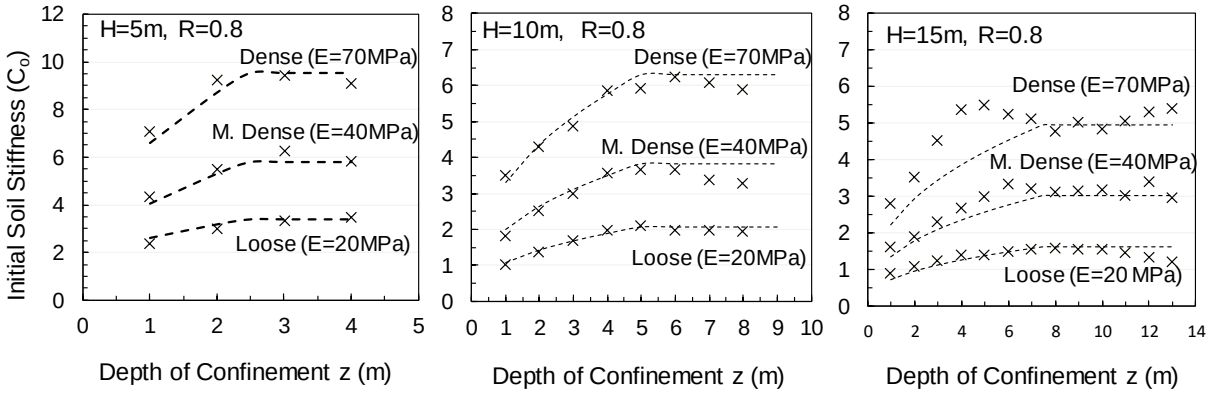

Fig. 15 C_o model (Eq. (7)) versus C_o extracted from FE analysis

H_{eff} is the wall height multiplied by a correction fraction 1/n that is as a function of the density of the backfill. For loose soil, the calibration yielded n=0.9. For medium-dense soil, n increases to 1.0 and for dense soil, n is equal to 1.1. In line with the findings established in the previous section, the simplified model in Eq. (7) expresses C_o as a function of the modulus of elasticity, the embedment depth, and the wall height. The parameter m is the same as that used in the soil hardening model (see Table 1). To test the effectiveness of Eq. (7), the FE-derived and the predicted C_o values were determined and plotted in Fig. 15 for cases with different wall heights. In Fig.15, the FE results are the "crosses" while the model predictions are the dashed lines. Results indicate that the simplified model (Eq. (7)) is capable of predicting C_o with an acceptable level of reliability. The only exception is the case involving a 15 m wall retaining dense soil, where the model slightly under predicts C_o for depths ranging from 3 to 6 m. For all practical purposes, it could be concluded that the two-segment model (Fig. 15) provides acceptable predictions of the variation of C_o with depth, relative density, and wall height.

5. Validation

In this section, the effectiveness of the hyperbolic p-y model presented in Eq. (3) is investigated for all representative cases analysed in this study. In predicting the passive p-y response using Eq. (3), the limit state passive pressure at any given depth is predicted using the Liu *et al.* model in Eq. (7), and R_f is assumed to be equal to 0.9.

The predicted (Eq. (3)) versus numerical (PLAXIS) passive p-y curves for four representative cases involving walls with heights ranging from 5 m to 15 m and soils with different relative densities are presented in Fig. 16. The analyzed cases include walls with different interface friction angles as reflected in R values ranging from 0.6 to 1.0. It is clear from Fig. 16 that the hyperbolic passive p-y expression that is depicted in Eq. (3) is capable of modeling the p-y response of rigid basement walls that retain granular soils of different relative densities.

The predictive performance portrayed in Fig. 16 is indicative of all other cases analyzed in this study (not shown for brevity). The parameters required to define the p-y relationship at different depths are limited to the limit state passive pressure as predicted by Liu *et al.* (2017) and the initial slope of the hyperbolic function as defined in Eq. (7). The proposed simplified passive hyperbolic p-y model that is presented in Eq. (3) (Ramberg-Osgood model) could be effectively employed to model the at-rest to passive segment of the p-y curves for rigid basement walls.

6. Conclusions

In this paper, finite element analyses were conducted to model the mobilization of passive earth pressures behind rigid basement walls. The intent is to investigate the possibility of generating p-y relationships that could be used

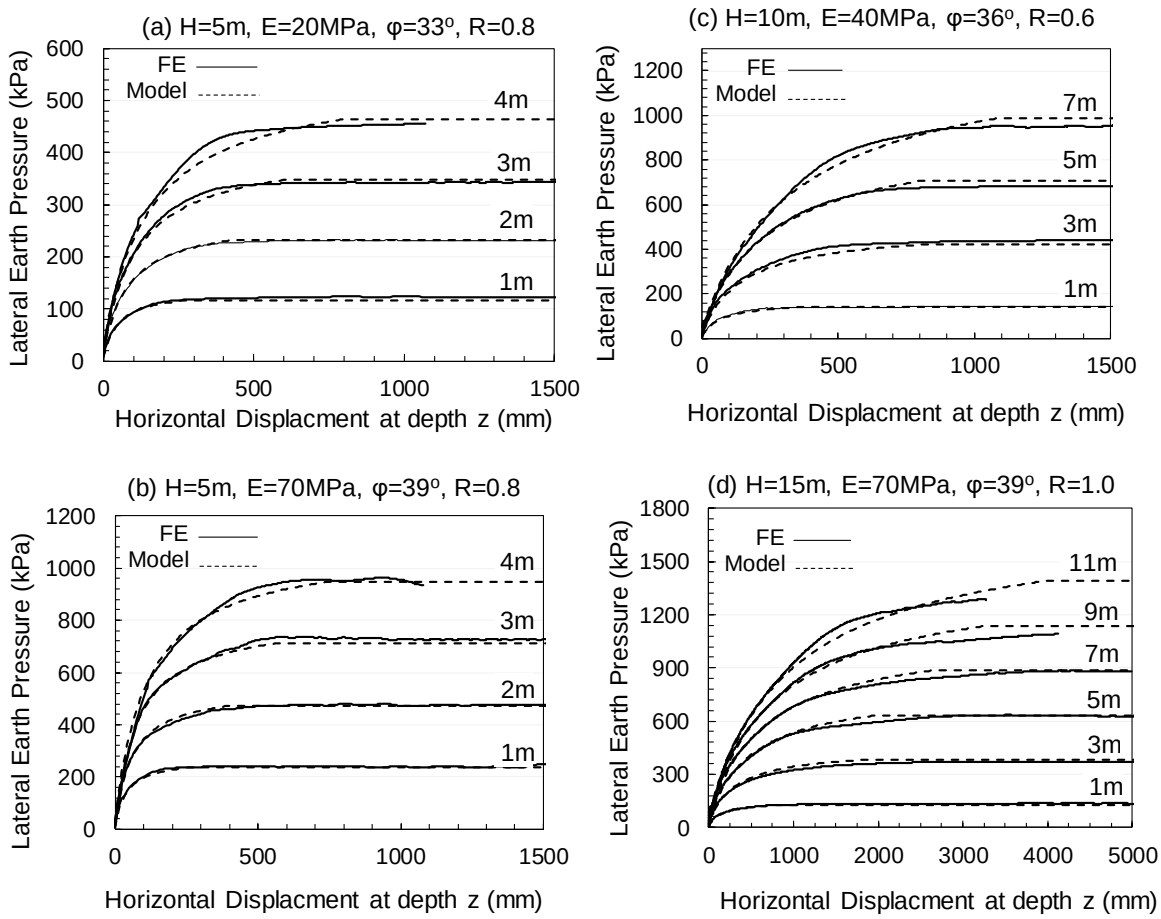

Fig. 16 Comparison between FE analysis and proposed model

in modeling soil response analogous to those used in pile analysis and design.

Based on the work, the following conclusions are made:

- The use of the Hardening soil model in the FE analysis resulted in p-y relationships that are realistic. The resulting p-y relationships at different depths were found to be sensitive to the relative density of the soil and the height of the wall, which had a direct effect on the magnitude of the local displacements required for passive conditions to be mobilized. Results showed that the 13mm displacement criterion that is typically referenced in the literature for the mobilization of passive conditions in p-y curves is not realistic for full scale rigid walls.
- The passive p-y response is affected by the depth below the ground surface z, the soil modulus E, the relative density, and the height of the wall H_w. On the other hand, the effect of the interface reduction factor R is confined to the p-y response at larger wall displacements.
- The passive p-y response could be accurately predicted using a hyperbolic model that is based on the Ramberg-Osgood equation which requires two parameters (passive pressure at limit state and initial stiffness C_o). The method by Liu *et al.* (2017) was found to be capable of predicting the numerically derived limit state passive pressures with an acceptable degree of accuracy. On the other hand, a simplified empirical model was derived to express the initial stiffness C_o as a function of the depth below the surface, modified height of wall, and modulus of elasticity. The proposed hyperbolic model was shown to yield reliable predictions of the passive p-y response for all the cases analyzed in this study.

It should be noted that the intent of this study is to provide a methodology for modeling passive p-y curves for cohesionless soils that are used as backfill behind rigid basement walls. In the finite element analyses that were conducted, the soil properties that were used pertain to those of Ottawa sand. As a result, the numerical results and the associated simplified model parameters are expected to be affected by the choice of the soil type used. Moreover, while the choice of the hardening soil model is adequate for loose and medium dense sands that do not exhibit significant post-peak softening in the stress-strain relationship, its use is questionable for dense sands that exhibit significant dilation and softening at large strains. The use of the hardening soil model for dense sands is a limitation that needs to be investigated in future studies.

Finally, it is worth mentioning that the problem under consideration in this study was tackled in a pseudo-static approach to try to characterize the "stiffness" of the springs that could be used to model the soil behind the wall. The stiffness is the main parameter that is required in properly modelling the soil behavior with springs. Modelling the dynamic effects is beyond the scope of this paper as it

requires that all factors that are related to damping be included in the analysis. The incorporation of damping is a separate study that could be done in the future to characterize the properties of the "dashpots" that will model the dynamic response of the soil together with the "springs".

Acknowledgments

The authors would like to acknowledge the support of the University Research Board (URB) at the American University of Beirut for funding this work.

References

Allotey, N. and El Naggar, M.H. (2007), "Generalized dynamic Winkler model for nonlinear soil-structure interaction analysis", *Can. Geotech. J.*, **45**(4), 560-573. https://doi.org/10.1139/T07-106.

American Petroleum Institute (1993), "API Recommended Practice for Planning, Designing, and Constructing Fixed Offshore".

Bakr, S. and Ahmad, S.M. (2018), "A finite element performance-based approach to correlate movement of a rigid retaining wall with seismic earth pressure", *Soil Dyn. Earthq. Eng.*, **114**, 460-479. https://doi.org/10.1016/j.soildyn.2018.07.025.

Boulanger, R.W., Curras, C.J., Kutter, B.L., Wilson, B.W. and Abghari, A. (1999), "Seismic soil-pile-structure interaction experiments and analysis", *J. Geotech. Geoenviron.*, **125**(9), 750-759. https://doi.org/10.1061/(ASCE)1090-0241(1999)125:9(750).

Briaud, J.L. and Kim, N.K. (1998), "Beam-column method for tieback walls", *J. Geotech. Geoenviron.*, **124**(1), 67-79. https://doi.org/10.1061/(ASCE)1090-0241(1998)124:1(67).

Chen, W.F. (1975), "Limit analysis and soil plasticity", Elsevier Science Publishers, B.V., Amsterdam, the Netherlands.

Clough, G.W. and Duncan, J.M. (1971), "Finite element analyses of retaining wall behavior", *J. Soil Mech. Found. Div.*, **97**(12), 1657-1673.

Conte, E., Troncone, A. and Vena, M. (2017). "A method for the design of embedded cantilever retaining walls under static and seismic loading", *Geotechnique*, **67**(12), 1081-1089. https://doi.org/10.1680/jgeot.16.P.201.

Coulomb, C.A. (1776), "An attempt to apply the rules of maxima and minima to several problems of stability related to architecture", *Mémoires de l'Académie Royale des Sciences*, **7**, 343-382.

Dilmac, H., Ulutas, H., Tekeli, H. and Demir, F. (2018). "The investigation of seismic performance of existing RC buildings with and without infill walls", *Comput. Concrete*, **22**(5), 439-447. https://doi.org/10.12989/cac.2018.22.5.439.

Duncan, J.M. and Chang, C.Y. (1970), "Non-linear analysis of stress and strain in soils", *J. Soil Mech. Found. Div.*, **96**(5), 1629-1653.

Duncan, J.M. and Mokwa, R.L. (2001), "Passive earth pressures: theories and tests", *J. Geotech. Geoenviron.*, **127**(3), 248-257. https://doi.org/10.1061/(ASCE)1090-0241(2001)127:3(248).

El Ganainy, H. and El Naggar, M.H. (2009), "Seismic performance of three-dimensional frame structures with underground stories", *Soil Dyn. Earthq. Eng.*, **29**(9), 1249-1261. https://doi.org/10.1016/j.soildyn.2009.02.003.

Elchiti, I., Saad, G., Najjar, SS. and Nasreddine, N. (2017), "Investigation of active soil pressures on retaining walls using finite element analyses", *Proceedings of the GeoFrontiers Conference,* March 12-15, Orlando, Florida, USA. https://doi.org/10.1061/9780784480458.016.

Gazetas, G., Garini, E. and Zafeirakos, A. (2016), "Seismic analysis of tall anchored sheet-pile walls", *Soil Dyn. Earthq. Eng.*, **91**, 209-221. https://doi.org/10.1016/j.soildyn.2016.09.031.

Hanna, A. and Diab, R. (2017), "Passive earth pressure of normally and over-consolidated cohesionless soil in terms of critical-state soil mechanics parameters", *Int. J. Geomech.*, **17**(1), 04016028. https://doi.org/10.1061/(ASCE)GM.1943-5622.0000683.

Hanna, A., Rahman, F. and Ayadat, T. (2011), "Passive earth pressure on embedded vertical plate anchors in sand", *Acta Geotechnica,* **6**(1), 21-29. https://doi.org/10.1007/s11440-010-0109-0.

Kumar, J. (2001), "Seismic passive earth pressure coefficients for sands", *Can. Geotech. J.*, **38**(4), 876-881. https://doi.org/10.1139/t01-004.

Liu, S., Xia, Y. and Liang, L. (2018), "A modified logarithmic spiral method for determining passive earth pressure", *J. Rock Mech. Geotech. Eng.*, **10**(6), 1171-1182. https://doi.org/10.1016/j.jrmge.2018.03.011.

Maleki, S. and Mahjoubi, S. (2010), "A new approach for estimating the seismic soil pressure on retaining walls", *Scientia Iranica*, **17**(4), 273-284.

Matlock, H. (1970), "Correlations for design of laterally loaded piles in soft clay", *Proceedings of the 2nd Annual Offshore Technology Conference*, OTC 1204, Houston, Texas. https://doi.org/10.4043/1204-MS.

Mikola, R.G., M.R., Candia, G. and Sitar, N. (2016). "Seismic earth pressures on retaining structures and basement walls in cohesionless soils", *J. Geotech. Geoenviron.*, **142**(10), 04016047. https://doi.org/10.1061/(ASCE)GT.1943-5606.0001507.

Ramberg, W. and Osgood, W.R. (1943), "Description of stress-strain curves by three parameters", Tech. Note 902, National Advisory Comm. Aeronaut., Washington, DC.

Rankine, W.J.M. (1857), "On the stability of loose earth", Philosophical Transaction of the Royal Society, London, UK.

Rao, K.S.S. and Choudhury, D. (2005), "Seismic passive earth pressures in soils", *J. Geotech. Geoenviron.*, **131**(1), 131-135. https://doi.org/10.1061/(ASCE)1090-0241(2005)131:1(131).

Reese, L.C., Cox, W.R. and Koop, F.D. (1974), "Analysis of laterally loaded piles in sand", *Proceedings of the 6th Offshore Technology Conference*, OTC 2080, Houston, Texas.

Richard, R.J., Huang, C. and Fishman, K.L. (1999). "Seismic earth pressure on retaining structures", *J. Geotech. Geoenviron.*, **125**(9), 771-778. https://doi.org/10.1061/(ASCE)1090-0241(1999)125:9(771).

Saad, G., Najjar, S.S. and Saddik, F. (2016), "Seismic performance of reinforced concrete shear wall buildings with underground stories", *Earthq. Struct.*, **10**(4), 965-988. https://doi.org/10.12989/eas.2016.10.4.965.

Skeini, H. (2015), "Numerical modeling of triaxial tests on clays with sand-column inclusions", Master Thesis, American University of Beirut.

Soubra, A.H. and Regenass, P. (2000), "Three-dimensional passive earth pressures by kinematical approach", *J. Geotech. Geoenviron.*, **126**(11), 969-978. https://doi.org/10.1061/(ASCE)1090-0241(2000)126:11(969).

Tejchman, J., Bauer, E. and Tantono, S.F. (2007), "Influence of initial density of cohesionless soil on evolution of passive earth pressure", *Acta Geotechnica*, **2**(1), 53. https://doi.org/10.1007/s11440-007-0022-3.

Terzaghi, K. (1943), "Theoretical soil mechanics", John Wiley and Sons 1943, New York, USA.

Wilson, D.W., Boulanger, R.W. and Kutter, B.L. (2000), "Observed seismic lateral resistance of liquefying sand", *J. Geotech. Geoenviron.*, **126**(10), 898-906. https://doi.org/10.1061/(ASCE)1090-0241(2000)126:10(898).

CC